Fast Deuterium Access to the Buried Magnesium/Manganese Site in Cytochrome *c* Oxidase†

Laurence Florens,‡,§,⊥ Bryan Schmidt,‡,§,|| John McCracken,*,|| and Shelagh Ferguson-Miller*,§

Departments of Biochemistry and Chemistry, Michigan State University, East Lansing, Michigan 48824

Received January 18, 2001; Revised Manuscript Received May 3, 2001

ABSTRACT: The recently determined crystal structures of bacterial and bovine cytochrome *c* oxidases show an area of organized water within the protein immediately above the active site where oxygen chemistry occurs. A pathway for exit of protons or water produced during turnover is suggested by possible connections of this aqueous region to the exterior surface. A non-redox-active Mg^{2+} site is located in the interior of this region, and our previous studies [Florens, L., Hoganson, C., McCracken, J., Fetter, J., Mills, D., Babcock, G. T., and Ferguson-Miller, S. (1998) in *Phototropic Prokaryotes* (Peschek, G. A., Loeffelhard, W., and Schmetterer, G., Eds.) Kluwer Academic/Plenum, New York] have shown that the protons of water molecules that coordinate the metal can be exchanged within minutes of mixing with ^2H_2O. Here we examine the extent and rate of deuterium exchange, using a combination of rapid freeze−quench and electron spin echo envelope modulation (ESEEM) analysis of Mn^{2+}-substituted cytochrome *c* oxidase, which retains full activity. In the oxidized enzyme at room temperature, deuterium exchange at the Mn^{2+} site occurs in less than 11 ms, which corresponds to an apparent rate constant higher than 3000 s^{-1}. The extent of deuterium substitution is dependent on the concentration of ^2H_2O in the sample, indicative of rapid equilibrium, with three inner sphere ^2H_2O exchanged per Mn^{2+}. This indicates that the water ligands of the Mn^{2+}/Mg^{2+} site, or the protons of these waters, can exchange with bulk solvent at a rate consistent with a role for this region in product release during turnover.

Cytochrome *c* oxidase is the terminal enzyme in the electron transport chains of most aerobic organisms. At the active site, electrons donated by cytochrome *c* are used to reduce dioxygen to two water molecules in an exothermic reaction. In addition to the four protons required for oxygen reduction, the energy gained from the reaction is used to transport an additional four protons across the membrane. The resulting electrochemical gradient produced by this proton translocation is later used in ATP synthesis.

High-resolution crystal structures of bacterial (*1*) and bovine (*2*) cytochrome *c* oxidases specify a similar spatial organization of the metal centers (Figure 1) and define some possible routes for proton translocation within the molecule via hydrogen-bonded paths. Several pathways for protons and water are expected in cytochrome *c* oxidase: on the inside of the membrane, entry pathways for protons to be pumped and for substrate protons required for oxygen reduction; on the outside of the membrane, an exit route for pumped protons and water. Candidates for the entry pathways have been identified by mutational and structural analysis (*3*−*5*), but the exit path remains unclear. A possible water channel which could serve this function was noted in the original bovine oxidase X-ray structure (*6*) (Figure 1) immediately above the active site, at the interface of subunits I and II. We proposed that this aqueous region could provide a proton and/or water exit pathway and further that control of its directionality could regulate the rate and the efficiency of coupling of cytochrome *c* oxidase (*7*). However, increasingly high-resolution structures indicate that water in this region is highly ordered, as indicated by low *B*-values at high and low temperatures, and therefore not likely to exchange readily or conduct protons (S. Yoshikawa, personal communication). Further, it is clear that unrestricted proton exchange between the outside and the active site would short-circuit the proton pumping mechanism of the enzyme. To understand the mechanism of proton translocation, the boundary defining the "outside" (or region of free access to solvent) in cytochrome oxidase needs to be determined (*8*).

A non-redox-active Mg^{2+} ion lies at the bottom of the proposed water channel, 12 Å from the surface of the protein. It bridges subunits I and II, shares a ligand with the binuclear Cu_A center, and is bonded through a histidine ligand and a water to the D-ring propionate of heme a_3. The role of the Mg^{2+} site is not known. However, its proximity to the apparent water channel suggests a function in determining the structure and the regulation of a proton and/or water exit pathway (*7*).

EPR[1] studies on *Rhodobacter sphaeroides* cytochrome *c* oxidase showed that manganese can be substituted for magnesium during growth of the bacterium (*9*) with no functional effect. Three out of six ligands for the Mg^{2+}/Mn^{2+} ion are provided by crystallographically well-defined water

† Supported by American Heart Association-Michigan Research Fellowship 9804540 (L.F.) and NIH Grants GM 26196 (S.F.-M.) and P01-GM 57323 (S.F.-M. and J.M.).

* Corresponding authors. S.F.-M.: fax, 517-353-9334; e-mail, fergus20@pilot.msu.edu. J.M.: fax, 517-353-1739; e-mail, mccracke@pilot.msu.edu.

‡ Both authors contributed equally to this work.

§ Department of Biochemistry.

⊥ Current address: Department of Cell Biology, The Scripps Research Institute, La Jolla, CA 92037.

|| Department of Chemistry.

10.1021/bi0101188 CCC: $20.00 © 2001 American Chemical Society
Published on Web 06/01/2001

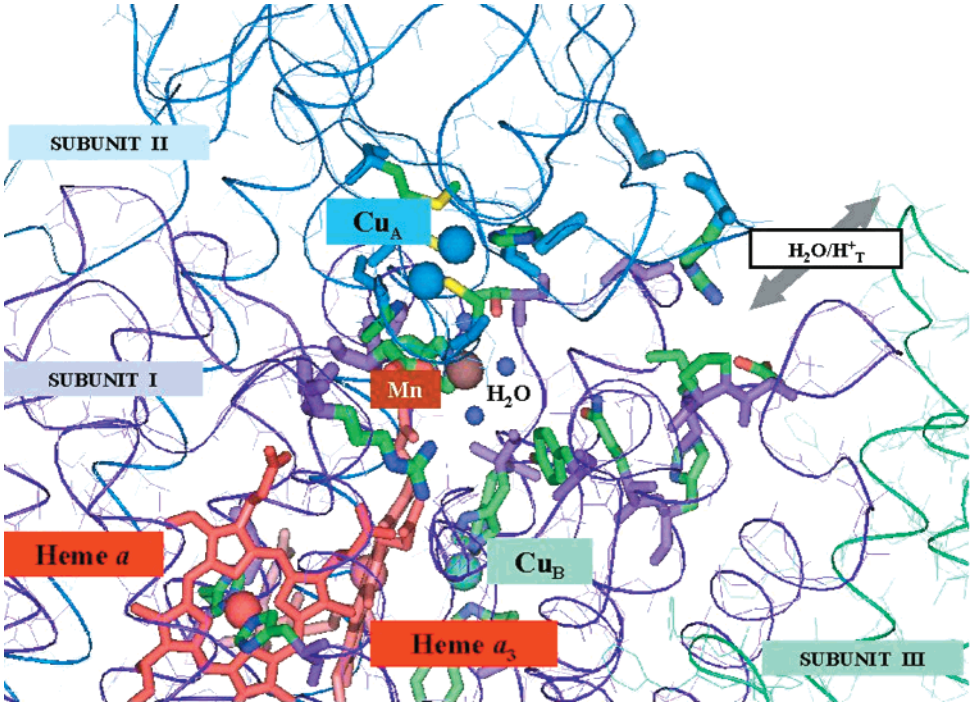

FIGURE 1: Metal centers and proposed water channel at the subunit I and II interface in the beef heart cytochrome *c* oxidase. Blue ribbons on the top are from subunit II and contain the dinuclear Cu_A site (larger light blue spheres). To the far right, in green ribbons, is subunit III, which contains no metal centers and does not directly contribute to the proposed water channel. The purple ribbons represent subunit I, the largest subunit, which contains the two hemes (in red) and Cu_B (light green sphere). The proposed water channel is shown as the gap between subunits I and II, beginning near the heme a_3 propionates and the Mg/Mn site (brown sphere), with residues lining the channel in stick form. The three crystallographically defined water ligands of manganese are represented by small blue spheres. Crystal structures of bacterial cytochrome *c* oxidases show a similar channel.

molecules. The paramagnetic nature of Mn^{2+} allows the use of the advanced EPR methods of electron nuclear double resonance spectroscopy (ENDOR) and ESEEM (*10*) to detect its ligation structure, and changes in structure, through the measurement of ligand hyperfine coupling.

In the present study, we have combined spectral (ESEEM) and kinetic (rapid freeze−quench) methods to measure the time scale and extent of deuterium exchange at the Mg^{2+}/Mn^{2+} site. The studies provide evidence of rapid water and/or proton exchange at least to the depth of the Mg^{2+}/Mn^{2+} site.

EXPERIMENTAL PROCEDURES

Protein Production and Purification. The amount of Mn^{2+} incorporated into the protein has been shown to depend on the [Mg^{2+}] to [Mn^{2+}] ratio in the growth medium (*9*). The YZ-300 strain (*11*) of *R. sphaeroides*, which overexpresses the wild-type cytochrome *c* oxidase with a histidine tag added to the C-terminus of subunit I, was grown on "high Mn" medium (with $MnSO_4$ and $MgSO_4$ at final concentrations of 700 and 50 μM, respectively). The protein was purified by Ni^{2+}-NTA affinity chromatography (*12*) and used with no further purification steps. The enzyme was concentrated and washed into buffer containing 50 mM KH_2PO_4−KOH, pH 7.4, 0.1 mM EDTA, and 0.1% lauryl maltoside, using a centrifugal filter (Millipore Ultrafree filter) with a 50 kDa nominal molecular mass limit. The visible spectral characteristics of the Mn^{2+}- and Mg^{2+}-substituted wild-type enzymes were identical, and oxygen consumption activities were unaltered (*9*).

Rapid-Mix Freeze−Quench ^2H_2O Exchange. The samples were prepared using an Update Instruments System 1000 chemical/freeze−quench apparatus (Model 715 Ram Controller and Model 1019 Syringe Ram). Two syringes of equal volume containing 60 μM cytochrome *c* oxidase in buffer A (50 mM KH_2PO_4−KOH, pH 7.4, 0.1 mM EDTA, 0.1% lauryl maltoside) and varying concentrations of deuterium oxide (99.9 atom % D, Aldrich), respectively, were maintained either at room temperature or in a water bath at 4 °C. The syringe contents were combined in a Wiskind grid mixer (model 1155) at a ram velocity of 1.25 cm•s^{-1}. Different reaction times were achieved either by varying the length of the tubing (aging hose) connecting the mixer to the spray nozzle or, for reaction times longer than 500 ms, by using the delay setting with a constant hose length (with the hose volume corresponding to the volume to be collected). The reaction mix was ultimately sprayed from a 0.008 in. diameter spray nozzle into a 4.5 in. long fused quartz EPR tube equipped with a funnel filled with cold isopentane (HPLC grade, Sigma), which quenches the reaction in approximately 5 ms (A.-L. Tsai, personal communication). The EPR tube and funnel were filled with isopentane and equilibrated for at least 5 min in an 8 L isopentane bath maintained at −140 ± 2 °C with a LakeShore Model 340 temperature controller equipped with a copper-constant thermocouple by an external liquid nitrogen bath. The frozen crystals of oxidase were packed into the bottom of the EPR tube by using a precooled packing rod until a densely packed

[1] Abbreviations: EDTA, ethylenediaminetetraacetic acid; ENDOR, electron nuclear double resonance; EPR, electron paramagnetic resonance; ESE, electron spin echo; ESEEM, electron spin echo envelope modulation; FT, Fourier transform.

sample with a height of at least 1 cm was obtained. The final concentration of cytochrome *c* oxidase in the EPR tube was measured to be approximately 10 μM. The freeze−quenched samples were stored in liquid nitrogen until analyzed by ESEEM. More recent studies were carried out using a starting enzyme concentration of 120 μM, giving a final concentration in the EPR tube of 30 μM, as indicated in figure legends, to increase the signal-to-noise ratio. Funnels and EPR tubes were also modified to use N_2 pressure to aid in the consistency of packing density, as described by Tsai et al. (*13*).

Electron Spin Echo Envelope Modulation (ESEEM). ESE-detected EPR and two- and three-pulse ESEEM spectra were recorded at 1.8 K by using a liquid helium immersion dewar under reduced (∼10 mbar) pressure on a pulsed spectrometer constructed at Michigan State University (*14*). Processing of experimental ESEEM data and Fourier transformations (FTs) were performed using Matlab software from Matworks Inc. (Natick, MA). The final 10 points of each time-domain data set were acquired with the integration window positioned 200 ns off of the echo to define the background. Spectra were normalized from zero (background) to one (maximum amplitude) before processing. Since the ESEEM of a discrete paramagnetic center is the product of echo modulations arising from each nucleus coupled to it (*15*, *16*), the ^{2}H modulations were isolated by dividing data obtained for cytochrome oxidase diluted in deuterated buffer by data obtained in a parallel fashion using aqueous buffer (*17*). Frequency spectra of ESEEM data were obtained using the dead-time reconstruction technique described by Mims (*18*). Imperfections in dead-time reconstruction led to baseline roll, or distortions, seen in the FTs. To gauge how the reconstruction procedure influenced the ^{2}H modulation peak amplitudes, a power spectrum of each time-domain data set was taken without dead-time reconstruction and used to calculate error bars.

RESULTS

Rate of Deuterium Exchange. The ESE-detected EPR spectrum of wild-type cytochrome *c* oxidase purified from *R. sphaeroides* grown in high Mn^{2+} medium (Figure 2B) is a composite of contributions from the Cu_A center (peak near 3120 G) and the Mn^{2+} ion (broad absorbance spanning from 2800 to 3800 G). Figure 2A shows an ESE-detected EPR absorption spectrum of a sample of oxidase from *R. sphaeroides* grown in high Mg^{2+} medium, which contains only EPR-silent Mg^{2+}, that was taken under identical conditions. This control shows that, at the X-band microwave frequency used in our studies, the absorption from Cu_A was characterized by a sharp decrease at magnetic field strengths above 3150 G. Thus, the Mn^{2+} ESEEM signal was studied at 3400 G where there is still significant Mn^{2+} absorbance but no interference from the Cu_A signal.

For cytochrome *c* oxidase in nondeuterated buffer, the FT of three-pulse ESEEM experiments performed at 3400 G (Figure 3, 0 ms spectrum) shows a weak signal centered at the proton Larmor frequency typical of ambient water molecules (14.45 MHz). Peaks are also resolved at 1.9, 2.7, and 5 MHz. These low-frequency modulations were previously assigned to nitrogen modulation from the histidine ligand (H411) of the Mn^{2+} (*19*). No deuterium ESEEM, as

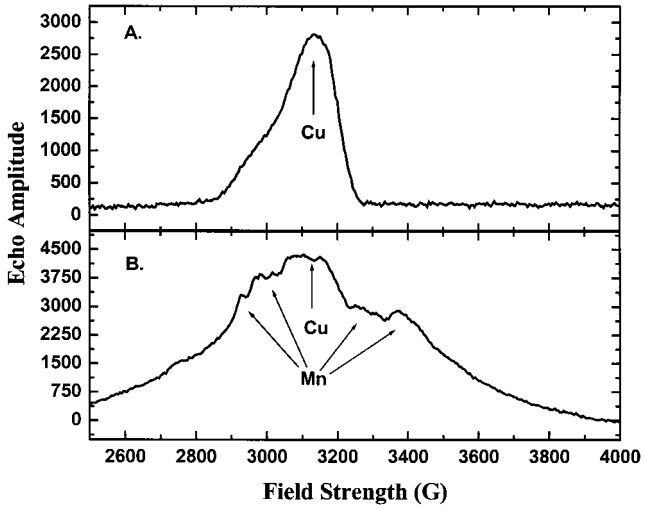

FIGURE 2: ESE-detected EPR spectra of cytochrome *c* oxidases with Mg^{2+} (A) or Mn^{2+} (B) incorporated into the metal site. Cytochrome *c* oxidase samples (ca. 30 μM final concentration) were diluted in deuterated buffer A and immediately transferred into EPR tubes and frozen in liquid nitrogen. Experimental conditions: ν = 8.870 GHz; power = 42 dBm; τ = 250 ns; 50 Hz pulse sequence repetition rate; 30 events per point; each scan contains 512 points; temperature = 1.8 K.

characterized by modulation at 2.2 MHz, was detected for the control sample. Also shown in Figure 3 are the results of parallel experiments performed on cytochrome *c* oxidase samples incubated with ^2H_2O for different lengths of time using the freeze−quench apparatus. The 11.4 ms spectrum of Figure 3 was characterized by an intense signal at the deuteron Larmor frequency (2.2 MHz), showing that within 11.4 ms protons magnetically coupled to the metal are exchanged for deuterons. When the sample was mixed in a 1:1 ratio with 100% ^2H_2O to give a final concentration of 50% ^2H_2O, the 2.2 MHz signal reached its maximum intensity during the dead time of the instrument (11.4 ms) and remained constant over a 10 s time course (Figure 3, 9800 ms spectrum). Assuming that the intensity of the 2.2 MHz peak as a function of mixing time is a single-exponential function, a lower limit exchange rate is calculated to be 3000 s^{-1}.

Number of Protons Exchanged. The X-ray crystal structures of cytochrome *c* oxidase indicate that three waters contribute to the ligation of the Mn^{2+}/Mg^{2+}. While the deuterium exchange data demonstrate that proton/deuteron exchange can occur on a catalytically relevant time scale, it does not by itself indicate the number of waters/protons exchanged.

To quantify the dependence of the extent of exchange on ^2H_2O concentration, a range of concentrations of ^2H_2O were mixed with the enzyme, resulting in final ^2H_2O enrichments of 15−75% (v/v). The intensity of the 2.2 MHz deuterium signal increased as ^2H_2O concentration increased, and a nonlinear relationship was observed between the echo amplitude and the ^2H_2O concentration (Figure 4). To extrapolate to the peak height for a sample with complete deuterium substitution (a D_2O concentration of 100%), a polynomial fit of the data was carried out. The best fit of the data was obtained with a cubic polynomial.

To estimate the number of exchanged waters/protons, manganese aquo, $Mn^{2+}(H_2O)_6$, was used as a standard. A

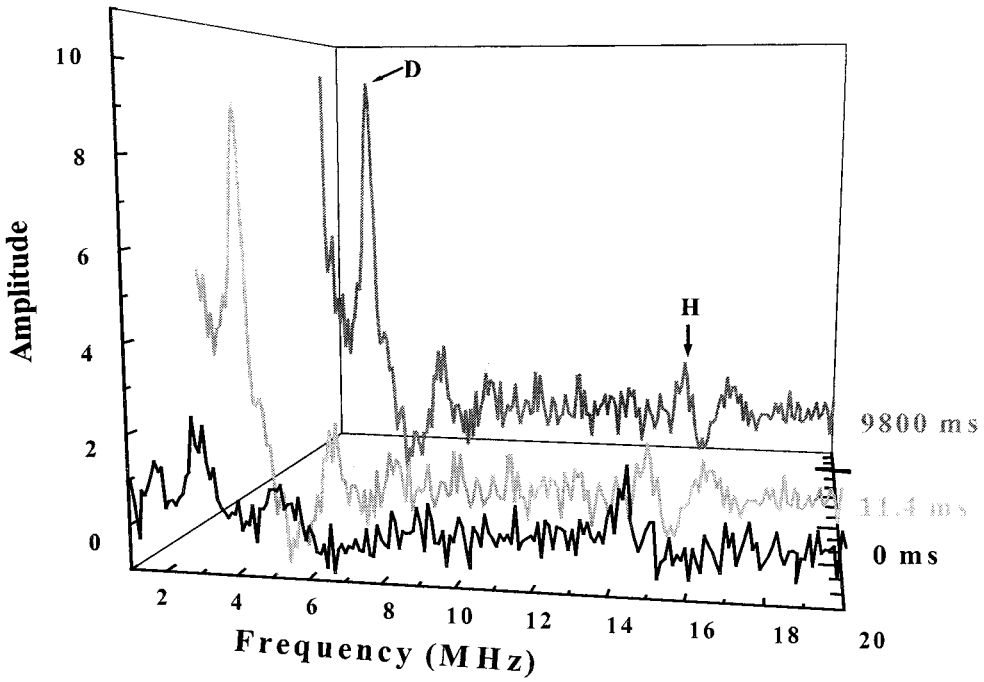

FIGURE 3: Fourier transforms of three-pulse ESEEM of cytochrome *c* oxidase samples, showing the contribution from deuterium exchange upon mixing into the Mn^{2+} binding site. Cytochrome *c* oxidase (ca. 60 μM, in buffer A) was rapidly mixed with ^2H_2O (1:1 volume ratio) at room temperature (ca. 20 °C) by using an Update Instruments freeze−quench apparatus and sprayed into an EPR tube containing cold isopentane (−140 °C) after 6.4 ms and 9.8 s mixing time. The cytochrome *c* oxidase concentration after packing was ca. 10 μM. For a $t = 0$ time reference point, a cytochrome *c* oxidase sample, at 10 μM in nondeuterated buffer A, was frozen in an EPR tube by immersion in liquid nitrogen. Experimental conditions: $\nu = 8.870$ GHz; $H_0 = 3400$ G; power = 42 dBm; $\tau = 200$ ns; $T = 40$ ns; 50 Hz pulse sequence repetition rate; 30 events per point; each scan contains 512 points collected in 10 ns increments; temperature = 1.8 K.

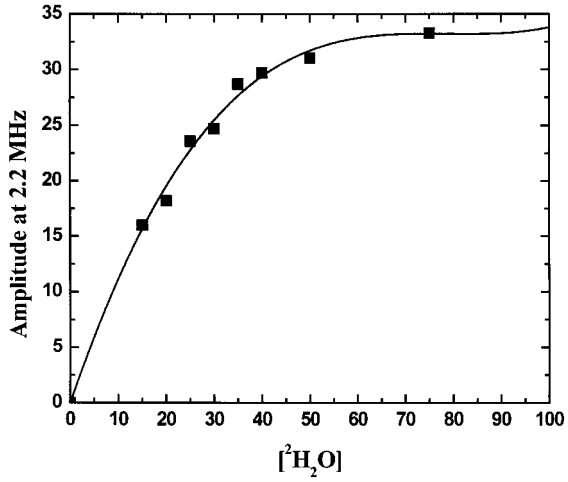

FIGURE 4: Fit of the Fourier transformations of two-pulse ESEEM spectra of wild-type oxidase incubated with various amounts of deuterium oxide. Samples were prepared as described in Figure 3, mixing with buffers with varying levels of ^2H_2O, which resulted in final concentrations of ^2H_2O ranging from 15% to 50%. The 75% final ^2H_2O concentration was obtained using a third syringe, containing 100% deuterated buffer, which was combined (using another mixer) with the aging hose (6.4 ms) containing the mixture of the first two syringes and incubated for an additional 8 ms. Plotting of the peak amplitude at 2.2 MHz versus ^2H_2O concentration was fitted to a cubic polynomial, as described in the text. Error bars were calculated as described in Experimental Procedures. Experimental conditions: $\nu = 8.870$ GHz; $H_0 = 3400$ G; power = 42 dBm; starting $\tau = 250$ ns; 50 Hz pulse sequence repetition rate; 30 events per point; each scan contains 512 points collected in 5 ns increments; temperature = 1.8 K.

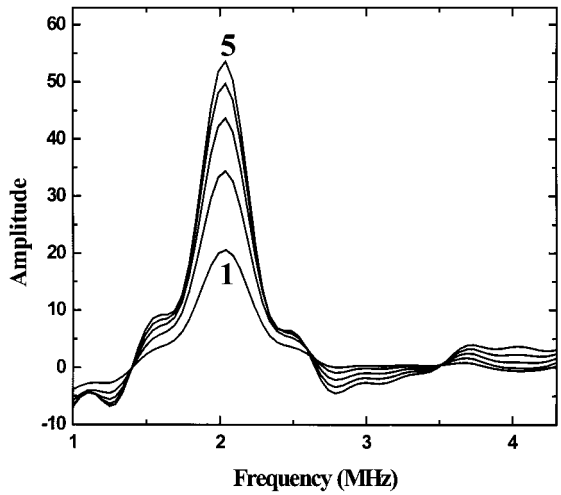

FIGURE 5: Fourier transformations of two-pulse ESEEM standard spectra of $Mn(H_2O)_6$ with increasing numbers of ^2H_2O bound to Mn^{2+}. The spectrum of one bound ^2H_2O (1) was obtained by taking the fifth root of a spectrum of a sample (5) containing 1 mM $MnSO_4$ dissolved in 80% ^2H_2O. Spectra for additional numbers of bound ^2H_2O were obtained by raising the one bound ^2H_2O spectrum to increasing powers. The final spectrum of five bound ^2H_2O (5) is the original spectrum acquired. Experimental conditions were as described in Figure 4 but with $\nu = 8.830$ GHz.

standard deuterated sample was prepared by dissolving 1 mM $MnSO_4$ in 100% ^2H_2O and adding glycerol to 40% (v/v) to ensure proper glassing. The final concentration of ^2H_2O in the standard can be calculated to be approximately 44 M, comprising 80% of the total water concentration.[2] Thus the spectrum [Figure 5 (5)] shows the contribution of five ^2H_2O molecules (80% of the six molecules that ligate the metal)

[2] Calculation of final ^2H_2O concentration was based on molar ratios of ^2H from ^2H_2O and ^1H from glycerol, assuming an exchange constant of approximately 1.

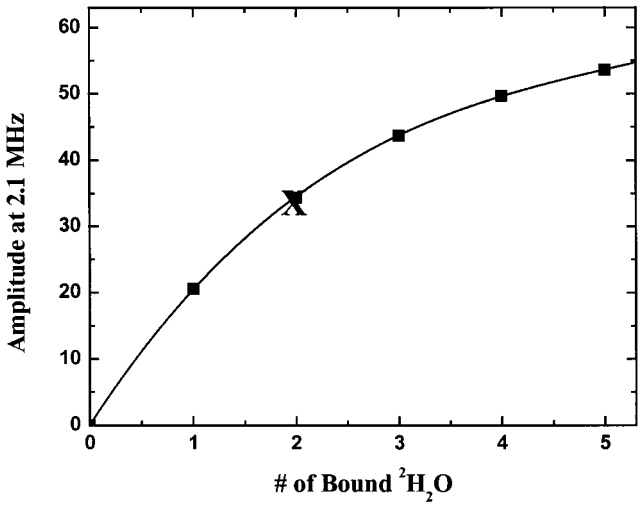

FIGURE 6: Fit of the amplitudes of the deuterium modulation peak at 2.2 MHz from the data sets shown in Figure 5 for the $Mn(H_2O)_6$ standard. The amplitudes are plotted versus the number of directly ligated ^2H_2O contributing to the spectrum. In addition to the directly ligated ^2H_2O, each point also has a contribution[3] from outer sphere ^2H_2O. For one bound ^2H_2O, there are approximately 22 outer sphere ^2H_2O, for two bound ^2H_2O there were approximately 43, for three bound ^2H_2O approximately 65, for four bound ^2H_2O approximately 87, and for five bound ^2H_2O approximately 108. The data were fit to a cubic polynomial. The X on the fit indicates the extrapolated 2.2 MHz peak height of oxidase in 100% ^2H_2O. Experimental conditions were as described in Figure 5.

ligated directly to the Mn^{2+} along with outer sphere ^2H_2O molecules. Since the total echo modulation is the product of each contributing nucleus, the fifth root of the spectrum gives the echo modulation of Mn^{2+} by one ^2H_2O ligand plus the region containing approximately one-sixth of the outer sphere deuterons [Figure 5 (1)]. Raising this spectrum to increasing powers (up to five) results in the spectrum of the echo modulation resulting from that number of bound ^2H_2O ligands and the associated outer sphere contribution. This can be used to create a standard curve for deuteron peak height at 2.2 MHz versus the number of bound ^2H_2O ligands (Figure 6). Comparing the height of the extrapolated 100% ^2H_2O peak from oxidase samples to this standard curve, we get an amplitude equivalent to approximately two bound ^2H_2O.

However, this number will be an underestimate of the waters at the Mn^{2+} in the protein, because the model, Mn^{2+}-$(^2H_2O)_6$, has a greater number of outer sphere ^2H_2O contributing to its modulation. Calculations reveal 130 water molecules contained within a 10 Å radius sphere of the metal in solution.[3] Thus, three bound ^2H_2O molecules in $Mn(H_2O)_6$ have an additional contribution from 65 outer sphere ^2H_2O molecules (see legend to Figure 6). Comparatively, high-resolution crystallographic analysis of bovine cytochrome *c* oxidase reveals that, in addition to the three bound waters, there are only 21 water molecules within 10 Å of the Mn^{2+} (S. Yoshikawa, personal communication). Additional evidence for the greater contribution of outer sphere waters in the echo modulation of the standard can be seen in the curves (Figures 4 and 6). Previous ESEEM studies of metal aquo complexes have shown that the outer sphere proton/deuteron contribution to the spectrum can be approximated as a linear addition (*20*, *21*). In contrast, deuterons in the first coordination sphere have a large contribution, and additional nuclei contribute to the 2.2 MHz peak amplitude in a multiplicative fashion. In the plot of ^2H modulation amplitude versus increasing ^2H_2O concentration for the protein (Figure 4), the curve clearly shows asymptotic behavior with 50% (v/v) ^2H_2O showing nearly maximal amplitude. This is indicative of minimal contribution of outer sphere deuterons to the echo modulation. However, the corresponding curve of the Mn^{2+}-$(^2H_2O)_6$ standard shows a more modest rise, or less of a "saturation" behavior, indicating a substantial contribution from outer sphere deuterons. The much smaller contribution of outer sphere deuterons to the amplitude of the signal from the oxidase Mn^{2+} site leads to an underestimation of the number of waters exchanged. We cannot calculate the extent of the underestimation with complete accuracy, but clearly our data imply that more than two Mn^{2+}-bound ^2H_2O molecules have exchanged by 11 ms after mixing. On the basis of the crystallographically defined ligands, we have an upper limit of three coordinating water molecules, indicating the likely exchange of all three.

Proton Movement through Ice. Previous studies have indicated that protons can move rapidly through an ice matrix with an estimated speed of 10^{-3} $cm^2/(V\cdot s)$ (*22*). This process could be problematic for our studies if deuterons are moving through the frozen enzyme even after rapid freezing, making time points for exchange of protons or deuterons at the Mn^{2+} site irrelevant. To determine if such an exchange is occurring, a sample was prepared by spraying a 120 μM oxidase solution and a 100% ^2H_2O solution simultaneously, but independently, into chilled isopentane, using the freeze–quench apparatus but bypassing the mixing step. Sample packing and storage were carried out in the same manner as for the samples for all other experiments. After 2 weeks of storage in liquid nitrogen, an ESEEM spectrum of the sample was taken. The spectrum shows no modulation at 2.2 MHz (Figure 7), indicating no deuterons had access to the Mn^{2+} either during the packing of the sample or during storage between sample preparation and acquisition of the spectrum.

DISCUSSION

The routes for proton uptake in cytochrome *c* oxidase are relatively well defined, but there is little evidence regarding the proton/water release pathway(s). Computer modeling and crystallographic structures indicate a large number of waters in the region above the hemes, but how rapidly these waters exchange with bulk solvent is a critical issue. The model of Wikström and colleagues (*23*) implies that when the protons are moved to the region above the hemes, they are already outside or have unhindered access to bulk solvent. Alternatively, the model of the Michel group (*24*) requires a location above the hemes where the proton can be trapped and inaccessible to bulk solvent. A third suggestion is that all of the waters seen in this area above the hemes are structural waters, and no rapid exchange can occur (S. Yoshikawa, personal communication). Further complicating the search for an exit route is the possibility of multiple or ill-defined

[3] The number of waters in a 10 Å radius sphere around a metal was calculated on the basis of molarity and density of water. The number of waters in a smaller sphere of 2.3 Å radius was calculated and subtracted from the larger sphere to account for the van der Waals volume of the metal. The six waters that are the direct ligands to the manganese aquo were also subtracted to yield the 130 waters calculated in the sphere.

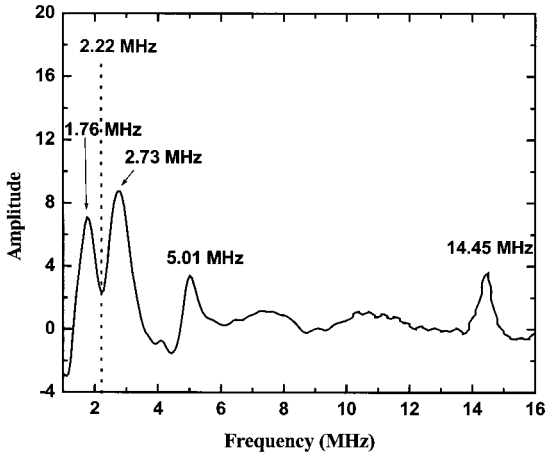

FIGURE 7: Exchangeability of protons at the manganese site at 77 K. Cytochrome *c* oxidase (120 μM) and 100% ^2H_2O were simultaneously but independently frozen in an EPR tube using the rapid freeze−quench method described above. The spectrum was acquired 15 days after sample preparation. Peaks at 1.76, 2.73, and 5 MHz arise from ^{14}N, while the peak at 14.45 MHz is due to protons. Modulation from deuterons is expected to occur at 2.22 MHz. Experimental conditions were as described in Figure 4.

pathways, as has been debated for the bacterial photosynthetic reaction center (*25, 26*).

Kinetic data on the rate of water exchange in proteins is difficult to obtain in complex enzymes such as cytochrome *c* oxidase. The Mn^{2+} ion, however, is spectrally accessible and conveniently located at the bottom of the putative water channel just above the active site, and thus it is a good probe of water flow in this region. ESEEM is the technique of choice to examine the magnetic nuclei in the vicinity of the Mn^{2+} ion because it can provide information regarding nuclei weakly coupled (such as ^1H and ^2H) to the transition metal. We used a freeze−quench apparatus for the preparation of samples to introduce rapid time resolution to the ESEEM experiments. Such freeze−quench techniques (*27*), combined with EPR spectroscopy, have been used for studying the appearance of radical intermediates in reaction mechanisms (*28*, *29*). The use of this technique to obtain the rate of water/proton flow in a protein has not been previously reported.

We define a lower limit of 3000 s^{-1} for the rate of the water/^2H_2O exchange at the Mn^{2+} site. When the cytochrome *c* oxidase is in its resting state (fully oxidized, not turning over), the maximal proton/deuterium exchange at the Mn^{2+} site occurs in less than 11.4 ms at room temperature and at 4 °C, which indicates that the protons of the water molecules in close association with the Mn^{2+} are in rapid equilibrium with the bulk solvent. These results support the concept that there is a kinetically relevant route for water or protons to exchange with bulk solvent to the depth of the water ligands of the Mg^{2+}/Mn^{2+} site. Because of the complex hydrogen-bonding network of waters around the Mn^{2+} in the protein, it is unclear where exactly water and/or protons are moving and by what routes they are accessing the Mn^{2+} site. However, the methodology established here provides a useful tool to test possible pathways by mutational analysis. The question of whether there is one pathway or whether this region is generally accessible to external solvent is an important current issue. Can subtle changes in the conformation of this region, which may occur during the oxygen chemistry at heme a_3-Cu_B, alter pK_a values and control accessibility, as in the case of bacteriorhodopsin (*30*)? In bacteriorhodopsin, a proton exit route involving hydrogen-bonded water and amino acid side chains exists in the resting state, but protons are not released until light induces a series of pK_a and conformational changes. Future studies using the rapid freeze−quench/ESEEM methodology will address these questions.

Although the molecular turnover of cytochrome oxidase can be as high as 2000 s^{-1} (giving a time constant of 0.5 ms), the 10 ms and longer time range that this method can sample is suitable for measuring deuterium exchange rates at the Mn^{2+} site during turnover in the 100 s^{-1} range often found in mutants, and it is ideal for determining if slow turnover of mutant forms is correlated with slowed movement of water or protons in this region. Hence, we have established a methodology combining rapid freeze−quench ^2H_2O exchange with ESEEM for measuring the kinetics of the water flow in the outer water/proton channel, providing an assay for mutants designed to reversibly or irreversibly block it.

ACKNOWLEDGMENT

We thank Dr. Shinya Yoshikawa (Himeji Institute, Japan) for generously communicating information about his X-ray crystal structure data prior to publication, Dr. Ah-Lim Tsai (University of Texas Medical School, Houston) for discussions regarding the optimization of the freeze−quench system, and Dr. Joan Broderick (Michigan State University) for the use of her freeze−quench apparatus.

REFERENCES

1. Iwata, S., Ostermeier, C., Ludwig, B., and Michel, H. (1995) *Nature (London) 376*, 660−669.
2. Tsukihara, T., Aoyama, H., Yashimata, E., Tomozaki, T., Yamaguchi, K. Shinzawa-Itoh, K., Nakashima, R., Yaono, R., and Yoshikawa, S. (1995) *Science 269*, 1069−1074.
3. Thomas, J. W., Puustinen, A., Alben, J. O., Gennis, R. B., and Wikström, M. (1993) *Biochemistry 32*, 10923−10928.
4. Fetter, J. R., Qian, J., Shapleigh, J., Thomas, J. W., Garcia-Horsman, A., Schmidt, E., Hosler, J., Babcock, G. T., Gennis, R. B., and Ferguson-Miller, S. (1995) *Proc. Natl. Acad. Sci. U.S.A. 95*, 1604−1608.
5. Zaslavsky, D., and Gennis, R. B. (2000) *Biochim. Biophys. Acta 1458*, 164−179.
6. Tsukihara, T., Aoyama, H., Yamashita, E., Tomizaki, T., Yamaguchi, H., Shinzawa-Itoh, K., Nakashima, R., Yaono, R., and Yoshikawa, S. (1996) *Science 272*, 1136−1144.
7. Ferguson-Miller, S., and Babcock, G. T. (1996) *Chem. Rev. 96*, 2889−2907.
8. Mills, D. A., Florens, L., Hiser, C., Qian, J., and Ferguson-Miller, S. (2000) *Biochim. Biophys. Acta 1458*, 180−187.
9. Hosler, J. P., Espe, M. P., Zhen, Y., Babcock, G. T., and Ferguson-Miller, S. (1995) *Biochemistry 34*, 7586−7592.
10. Atherton, N. M. (1993) *Principles of Electron Spin Resonance*, E. Horwood, Ltd., Chichester, England.
11. Zhen, Y., Qian, J., Follmann, K., Hayward, T., Nilsson, T., Dahn, M., Hilmi, Y., Hamer, A. G., Hosler, J. P., and Ferguson-Miller, S. (1998) *Protein Purif. Expression 13*, 326−336.
12. Mitchell, D. M., and Gennis, R. B. (1995) *FEBS Lett. 368*, 148−150.
13. Tsai, A.-L., Berka, V., Kulmacz, R. J., Wu, G., and Palmer, G. (1998) *Anal. Biochem. 262*, 1−7.
14. McCracken, J., Shin, D.-H., and Dye, J. L. (1992) *Appl. Magn. Reson. 3*, 305−316.
15. Rowan, L. G., Hahn, E. L., and Mims, W. B. (1965) *Phys. Rev. 137*, A61−A71.

16. Debanow, S. G., Shuben, A. G., and Parmon, V. N. (1981) *J. Magn. Reson. 42*, 474−487.
17. Mims, W. B., Davis, J. L., and Peisach, J. (1984) *Biophys. J. 45*, 755−766.
18. Mims, W. B. (1984) *J. Magn. Reson. 59*, 291−306.
19. Espe, M. P., Hosler, J. P., Ferguson-Miller, S., Babcock, G. T., and McCracken, J. (1995) *Biochemistry 34*, 7593−7602.
20. Mims, W. B., Peisach, J., and Davis, J. L. (1977) *J. Chem. Phys. 66*, 5536−5550.
21. Mims, W. B., and Davis, J. L. (1976) *J. Chem. Phys. 64*, 4836−4846.
22. Nagle, J. F., and Morowitz, H. J. (1978) *Proc. Natl. Acad. Sci. U.S.A. 75*, 298−302.
23. Puustinen, A., and Wikström, M. (1999) *Proc. Natl. Acad. Sci. U.S.A. 96*, 35−37.
24. Michel, H. (1999) *Biochemistry 38*, 15129−15140.
25. Paddock, M. L., Feher, G., and Okamura, M. Y. (2000) *Proc. Natl. Acad. Sci. U.S.A. 97*, 1548−1553.
26. Baciou, L., and Michel, H. (1995) *Biochemistry 34*, 7967−7972.
27. Ballou, D. P. (1978) *Methods Enzymol. 54*, 85−93.
28. Schultz, B. E., Edmondson, D. E., and Chan, S. I. (1998) *Biochemistry 37*, 4160−4168.
29. Padmakumar, R., and Banerjee, R. (1995) *J. Biol. Chem. 270*, 9295−9300.
30. Luecke, H., Schobert, B., Richter, H.-T., Cartailler, J.-P., and Lanyi, J. K. (1999) *Science 286*, 255−260.

BI0101188